SUPPLEMENTARY INFORMATION

Reduction of 1,2,3-Trichloropropane (TCP): Pathways and Mechanisms from Computational Chemistry Calculations

*Tifany L. Torralba-Sanchez[1], Eric J. Bylaska[2], Alexandra J. Salter-Blanc[3], Douglas E. Meisenheimer[1], Molly A. Lyon[1], and Paul G. Tratnyek[1]**

[1] OHSU-PSU School of Public Health, Oregon Health & Science University
3181 SW Sam Jackson Park Road, Portland, OR 97239

[2] William R. Wiley Environmental Molecular Sciences Laboratory, Pacific Northwest National Laboratory, P.O. Box 999, Richland, WA. 99352

[3] Jacobs, 2020 SW 4th Avenue, Suite 300, Portland, OR 97201

*Corresponding author: Email: tratnyek@ohsu.edu, Phone: 503-346-3431

Contents

Computational Method Details	S2
Reactions Modeled, from Figure 2 (Table S1)	S4
Free energies of reaction calculated with hydron (H^+) model (Table S2)	S6
Free energies of reaction calculated with hydronium (H_3O^+) model (Table S3)	S8
Comparison of hydron vs. hydronium modeling (Figure S1)	S10
Reaction coordinate diagrams with DFT methods (Figures S2-S5)	S11
Batch Experimental Methods	S15
Kinetic Data from batch experiments (Figures S6-S8)	S16
References for Supporting Information	S19

20 pages, 3 Tables, 8 Figures, 26 References

Computational Methods

All of the electronic structure calculations in this study were performed with the NWChem program suite. These calculations were performed at the density functional theory (DFT) and coupled-cluster theory (CCSD(T)), a wave function theory (WFT), levels. The Kohn−Sham equations of DFT were solved using the gradient-corrected B3LYP,[1, 2] PBE0,[3] PBE96[4], and M06-2X[5] exchange-correlation functionals. DFT calculations and CCSD(T) calculations[6, 7] were performed using the 6-311++G(2d,2p) basis set (all d-orbitals were Cartesian 6d). [8, 9] In these calculations, the geometries of the neutral and radical cation species were optimized first and then the vibrational frequencies were determined by using a finite difference approach. The free energies in the gas phase were determined using the gas-phase optimized structures and frequencies as input for free energy formulae derived from statistical mechanics.[10, 11]

Solvation energies for solutes were approximated as a sum of non-covalent electrostatic, cavitation, and dispersion energies (using the same methods we used in recent work on nitro reduction of energetic compounds[12]). The electrostatic contributions to the solvation energies were estimated by using the self-consistent reaction field theory of Klamt and Schüürmann (COSMO), [13] with the cavity defined by a set of overlapping atomic spheres with radii suggested by Stefanovich and Truong[14] (H– 1.172 Å, C– 2.096 Å, C= 1.635 Å, O– 1.576 Å, and Cl– 1.750 Å). The dielectric constant of water used for all of the solvation calculations was 78.4. [13] The cavitation and dispersion contributions to the solvation energy are less straight-forward to handle because the interactions take place at short distances, so several methods have been proposed to do this.[15-22] One of the simplest approaches for estimating these terms is to use empirically derived expressions that depend only on the solvent accessible surface area. In this study, the widely used formula of Sitkoff et al.[19] was used to augment the COSMO calculations,

$$\Delta G_{cav+disp} = \gamma A + b \qquad \text{(S1)}$$

where γ and b are constants set to 5 cal/mol-Å^2 and 0.86 kcal mol^{-1} respectively. Sitkoff et al. parameterized the constants γ and b to the experimentally determined free energies of solvation of alkanes[23] by using a least-squares fit. The Shrake-Rupley algorithm was used to determine the solvent accessible surface areas.[24] The calculated free energies of reaction with the addition of

an electron (e^-) in aqueous solution were referenced relative to the standard hydrogen electrode (SHE) using the absolute potential of SHE, E_H^0 = 98.6 kcal mol^{-1} = 4.28 V.

The EMSL Arrows scientific service was used to carry out and keep track of the large number of calculations (>500 calculations) used in this study. EMSL Arrows is a new scientific service (started in August 2016) that combines NWChem, SQL and NOSQL databases, email, and web APIs that simplifies molecular and materials modeling and can be used to carry out and manage large numbers of complex calculations with diverse levels of theories. The simplest input to EMSL Arrows is just a chemical reaction, where the reactants and products can be described as either a SMILES string, common name, IUPAC, KEGG numbers, CAS, PubChem ids, ChemSpider ids, or InChI strings. An example input is as follows,

C(C(CCl)Cl)Cl + [SHE] --> ClC[CH]CCl mult{2} + [Cl-] ~ xc{m06-2x}

in which EMSL Arrows produces results that are a combination of text and graphical output as shown below.

```
Reaction 1: C(C(CCl)Cl)Cl xc{m06-2x} + [SHE]  xc{m06-2x} -->  ClC[CH]CCl mult{2} xc{m06-2x} + [Cl-] xc{m06-2x}
 - instance 1: 1.00 (Id=44164) + 1.00 SHE ^{-1} --> 1.00 (Id=44188) + 1.00 (Id=40886)
 - instance 1: 1.00 1,2,3-trichloropropane + 1.00 SHE ^{-1} --> 1.00 1,3-dichloropropane doublet radical + 1.00 chlorane anion
 - instance 1: 1.00 C3Cl3H5 + 1.00 SHE ^{-1} --> 1.00 C3Cl2H5 + 1.00 Cl1
 - instance 1:   1.00 ClCC(CCl)Cl theory{dft} basis{6-311++G(2d,2p)} xc{m06-2x} solvation_type{COSMO} ^{0} mult{1} nf{0} + 1.00 SHE ^{-1}
 - instance 1:   --> 1.00 ClC[CH]CCl theory{dft} basis{6-311++G(2d,2p)} xc{m06-2x} solvation_type{COSMO} ^{0} mult{2} nf{0}
 - instance 1:     + 1.00 [Cl] theory{dft} basis{6-311++G(2d,2p)} xc{m06-2x} solvation_type{COSMO} ^{-1} mult{1} nf{0}
 - instance 1:        Erxn(gas)       Hrxn(gas)       Grxn(gas) Delta_Solvation        Grxn(aq)
 - instance 1:           -1.392          -3.522         -13.000         -80.720           4.879  -- in kcal/mol (electrode bias =  98.600 kcal/mol)
 - instance 1:           -5.826         -14.736         -54.393        -337.734          20.415  -- in kj/mol
 - instance 1:        -0.002219       -0.005613       -0.020717       -0.128636        0.007776  -- in Hartrees
```

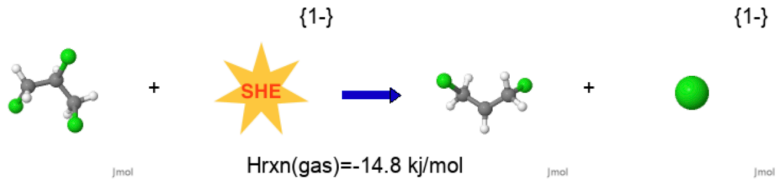

More information on EMSL Arrows can be found at the www.arrows.emsl.pnl.gov/api and http://www.nwchem-sw.org/index.php/EMSL_Arrows# websites.

Table S1. Balanced reactions for candidate TCP transformation pathways shown in Figure 2 in the main text.

Reaction ID No. [a]	Reaction Coordinate [a]	Balanced Reaction [a,b]	Reaction Name/Type [c]
1	1,2	1,2,3-TCP + e^- → INT1 + Cl^-	D1EA
2	3	INT1 + H^+ + e^- → 1,3-DCP	HA
3	4	INT1 + e^- → AC + Cl^-	D1EA
4	2	1,2,3-TCP + e^- → INT2 + Cl^-	D1EA
5	3	INT2 + H^+ + e^- → 1,2-DCP	HA
6	4	INT2 + e^- → AC + Cl^-	D1EA
7	4	TCP + $2e^-$ → AC + $2Cl^-$	BRE
8	4	1,3-DCP → AC + HCl	DHX
9	4	1,2-DCP → AC + HCl	DHX
10	5	AC + e^- → INT3 + Cl^-	D1EA
11	8	INT3 + H^+ + e^- → PrE	HA
12	5	1,3-DCP + e^- → INT4 + Cl^-	D1EA
13	6	INT4 + H^+ + e^- → 1-CP	HA
14	8	INT4 + e^- → PrE + Cl^-	D1EA
15	5	1,2-DCP + e^- → INT5 + Cl^-	D1EA
16	6	INT5 + H^+ + e^- → 2-CP	HA
17	8	INT5 + e^- → PrE + Cl^-	D1EA
18	8	1,2-DCP + $2e^-$ → PrE + $2Cl^-$	BRE
19	8	1,3-DCP + $2e^-$ → PrE + $2Cl^-$	BRE
20	5	1,2-DCP + e^- → INT6 + Cl^-	D1EA
21	6	INT6 + H^+ + e^- → 1-CP	HA
22	10	PrE + H_2 → PrA	HDG
23	9	1-CP + e^- → INT7 + Cl^-	D1EA
24	10	INT7 + H^+ + e^- → PrA	HA
25	9	2-CP + e^- → INT8 + Cl^-	D1EA
26	10	INT8 + H^+ + e^- → PrA	HA
27	3	1,2,3-TCP → 1,3-DCPrE + HCl	DHX
28	3	1,2,3-TCP → 1,2-DCPrE + HCl	DHX
29	5	1,3-DCPrE + e^- → INT9 + Cl^-	D1EA
30	6	INT9 + H^+ + e^- → 3-CPrE	HA

31	5	1,2-DCPrE + e^- → INT10 + Cl^-	D1EA
32	6	INT10 + H^+ + e^- → 2-CPrE	HA
33	7	3-CPrE + e^- → INT11 + Cl^-	D1EA
34	8	INT11 + H^+ + e^- → PrE	HA
35	7	2-CPrE + e^- → INT12 + Cl^-	D1EA
36	8	INT12 + H^+ + e^- → PrE	HA

[a] Reaction ID No. and Abbreviations correspond to those in Figure 2 in the main text. Reaction Coordinate indicates the pathway stage and corresponds to that of the main product of each reaction with the exception of Rxn 1, which also includes the Reaction Coordinate for TCP (i.e., 1).

[b] **1,2,3-TCP**: 1,2,3-trichloropropane; **INT1**: 1,3-dichloropropane doublet radical (13DCP•); **1,3-DCP**: 1,3-dichlorpropane; **AC**: allyl chloride (AChl); **INT2**: 1,2-dichloropropane doublet radical (12DCP•); **1,2-DCP**: 1,2-dichlorpropane; **INT3**: 1-propene doublet radical (1Pr•); **PrE**: propene; **INT4**: 3-chloropropane doublet radical (3CP•); **1-CP**: 1-chloropropane; **INT5**: 2-chloropropane doublet radical (2CP•); **2-CP**: 2-chloropropane; **INT6**: 1-chloropropane doublet radical (1CP•); **PrA**: propane; **INT7**: 1-propane doublet radical (1PrA•); **INT8**: 2-propane doublet radical (2PrA•); **1,3-DCPrE**: 1,3-dichloropropene; **1,2-DCPrE**: 1,2-dichloropropene; **INT9**: 3-chloropropene doublet radical (3CPrE•); **3-CPrE**: 3-chloropropene; **INT10**: 2-chloropropene doublet radical (2CPrE•); **2-CPrE**: 2-chloropropene; **INT11**: 3-propene doublet radical (3PrE•); **INT12**: 2-propene doublet radical (2PrE•).

[c] **D1EA**: Dissociative 1-Electron Attachment; **HA**: H-atom attachment; **BRE**: Reductive β-Elimination; **DHX**: Dehydrohalogenation; **HDG**: Hydrogenation.

Table S2. Computationally derived standard state aqueous phase Gibbs free energies of reactions (ΔG^0_{rxn} (aq), kcal/mol) for candidate TCP transformation pathways shown in Figure 2 in the main text. These electronic structure calculations were performed using the hydron (H^+) model for the H-atom attachment (HA) reactions.

Reaction ID No.[a]	Reaction in SMILES Format [b]	ΔG^0_{rxn} (aq) (kcal/mol)				
		Basis Set: 6-311++G(2d,2p)				
		Theory: DFT				Theory: CCSD(T)
		Exchange-Correlation Functional				
		B3LYP	PBE0	PBE96	M06-2X	
1	C(C(CCl)Cl)Cl + [SHE] --> ClC[CH]CCl mult{2} + [Cl-]	-6.021	2.683	2.489	4.879	9.962
2	ClC[CH]CCl mult{2} + [H+] + [SHE] --> C(CCl)CCl	-42.996	-42.465	-39.508	-43.965	-44.223
3	ClC[CH]CCl mult{2} + [SHE] --> C=CCCl + [Cl-]	-53.437	-45.942	-45.250	-50.769	-46.634
4	C(C(CCl)Cl)Cl + [SHE] --> [CH2]C(Cl)CCl mult{2} + [Cl-]	-1.372	6.555	7.052	7.486	12.075
5	[CH2]C(Cl)CCl mult{2} + [H+] + [SHE] --> CC(CCl)Cl	-48.479	-47.621	-45.541	-48.703	-48.348
6	[CH2]C(Cl)CCl mult{2} + [SHE] --> C=CCCl + [Cl-]	-58.086	-49.814	-49.812	-53.375	-48.747
7	C(C(CCl)Cl)Cl + 2 [SHE] --> C=CCCl + 2 [Cl-]	-59.457	-43.259	-42.760	-45.890	-36.672
8	C(CCl)CCl --> C=CCCl + HCl	-0.539	5.331	3.117	5.233	2.349
9	CC(CCl)Cl --> C=CCCl + HCl	0.294	6.616	4.588	7.365	4.361
10	C=CCCl + [SHE] --> C=C[CH2] mult{2} + [Cl-]	-10.648	-4.292	-2.422	-3.061	1.280
11	C=C[CH2] mult{2} + [H+] + [SHE] --> CC=C	-35.892	-34.093	-33.215	-36.256	-35.700
12	C(CCl)CCl + [SHE] --> [CH2]CCCl mult{2} + [Cl-]	3.340	9.402	10.690	10.144	14.376
13	[CH2]CCCl mult{2} + [H+] + [SHE] --> CCCCl	-50.163	-47.771	-46.605	-49.350	-48.643
14	[CH2]CCCl mult{2} + [SHE] --> CC=C + [Cl-]	-60.320	-51.264	-52.068	-56.265	-51.207
15	CC(CCl)Cl + [SHE] --> [CH2]C(C)Cl mult{2} + [Cl-]	-0.143	7.244	7.862	8.299	12.775
16	[CH2]C(C)Cl mult{2} + [H+] + [SHE] --> CC(C)Cl	-48.360	-46.927	-45.062	-48.583	-48.274

17	[CH2]C(C)Cl mult{2} + [SHE] --> CC=C + [Cl-]	-56.003	-47.821	-47.769	-52.288	-47.594
18	CC(CCl)Cl + 2 [SHE] --> CC=C + 2 [Cl-]	-56.147	-40.577	-39.907	-43.989	-34.819
19	C(CCl)CCl + 2 [SHE] --> CC=C + 2 [Cl-]	-56.980	-41.862	-41.378	-46.121	-36.831
20	CC(CCl)Cl + [SHE] --> C[CH]CCl mult{2} + [Cl-]	-2.495	4.101	4.778	5.831	12.517
21	C[CH]CCl mult{2} + [H+] + [SHE] --> CCCCl	-43.495	-41.185	-39.222	-42.906	-44.772
22	CC=C + [HH] --> CCC	-18.825	-24.344	-21.476	-20.407	-19.920
23	CCCCl + [SHE] --> [CH2]CC mult{2} + [Cl-]	4.751	10.944	12.477	11.462	15.599
24	[CH2]CC mult{2} + [H+] + [SHE] --> CCC	-49.539	-47.278	-46.378	-48.841	-48.168
25	CC(C)Cl + [SHE] --> C[CH]C mult{2} + [Cl-]	2.705	9.148	10.282	10.880	15.576
26	C[CH]C mult{2} + [H+] + [SHE] --> CCC	-44.979	-42.883	-41.427	-45.050	-44.901
27	C(C(CCl)Cl)Cl --> C(=CCl)CCl + HCl	-3.409	2.873	0.119	5.004	2.030
28	C(C(CCl)Cl)Cl --> C(=CCl)(C)Cl + HCl	-3.033	1.971	-0.840	3.841	1.255
29	C(=CCl)CCl + [SHE] --> [H][C]([H])C=CCl mult{2} + [Cl-]	-12.159	-5.910	-4.144	-4.817	-0.011
30	[H][C]([H])C=CCl mult{2} + [H+] + [SHE] --> C(=CCl)C	-34.953	-33.072	-31.912	-35.189	-34.785
31	C(=CCl)(C)Cl + [SHE] --> CC(Cl)=[CH] mult{2} + [Cl-]	11.438	19.111	20.313	18.384	22.438
32	CC(Cl)=[CH] mult{2} + [H+] + [SHE] --> C(=C)(C)Cl	-60.144	-58.583	-56.720	-59.199	-58.499
33	C(=CCl)C + [SHE] --> CC=[CH] mult{2} + [Cl-]	14.255	20.778	22.598	20.032	23.970
34	CC=[CH] mult{2} + [H+] + [SHE] --> CC=C	-59.830	-57.504	-56.198	-58.201	-57.537
35	C(=C)(C)Cl + [SHE] --> C[C]=C mult{2} + [Cl-]	10.855	17.516	18.770	18.059	22.794
36	C[C]=C mult{2} + [H+] + [SHE] --> CC=C	-55.211	-52.851	-51.061	-54.254	-54.320

[a] Reaction ID No. correspond to those in Figure 2 in the main text. Reaction details are described in Table S1.

[b] Syntax for submission to Arrows. [SHE]: Standard Hydrogen Electrode for electron e^-. mult{}: multiplicity or degeneracy. mult{2}: doublet radical. [HH]: H_2.

Table S3. Computationally derived standard state aqueous phase Gibbs free energies of reactions (ΔG^0_{rxn} (aq), kcal/mol) for candidate TCP transformation pathways shown in Figure 2 in the main text. These electronic structure calculations were performed using the hydronium (H_3O^+) model for the H-atom attachment (HA) reactions.

Reaction ID No.[a]	Reaction in SMILES Format [b]	ΔG^0_{rxn} (aq) (kcal/mol)				
		Basis Set: 6-311++G(2d,2p)				
		Theory: DFT				Theory: CCSD(T)
		Exchange-Correlation Functional				
		B3LYP	PBE0	PBE96	M06-2X	
1	C(C(CCl)Cl)Cl + [SHE] --> ClC[CH]CCl mult{2} + [Cl-]	-6.021	2.683	2.489	4.879	9.962
2	ClC[CH]CCl mult{2} + [OH3+] + [SHE] --> C(CCl)CCl + water	-54.847	-52.502	-51.072	-55.794	-54.738
3	ClC[CH]CCl mult{2} + [SHE] --> C=CCCl + [Cl-]	-53.437	-45.942	-45.250	-50.769	-46.634
4	C(C(CCl)Cl)Cl + [SHE] --> [CH2]C(Cl)CCl mult{2} + [Cl-]	-1.372	6.555	7.052	7.486	12.075
5	[CH2]C(Cl)CCl mult{2} + [OH3+] + [SHE] --> CC(CCl)Cl + water	-60.329	-57.658	-57.105	-60.532	-58.863
6	[CH2]C(Cl)CCl mult{2} + [SHE] --> C=CCCl + [Cl-]	-58.086	-49.814	-49.812	-53.375	-48.747
7	C(C(CCl)Cl)Cl + 2 [SHE] --> C=CCCl + 2 [Cl-]	-59.457	-43.259	-42.760	-45.890	-36.672
8	C(CCl)CCl --> C=CCCl + HCl	-0.539	5.331	3.117	5.233	2.349
9	CC(CCl)Cl --> C=CCCl + HCl	0.294	6.616	4.588	7.365	4.361
10	C=CCCl + [SHE] --> C=C[CH2] mult{2} + [Cl-]	-10.648	-4.292	-2.422	-3.061	1.280
11	C=C[CH2] mult{2} + [OH3+] + [SHE] --> CC=C + water	-47.742	-44.129	-44.779	-48.085	-46.215
12	C(CCl)CCl + [SHE] --> [CH2]CCCl mult{2} + [Cl-]	3.340	9.402	10.690	10.144	14.376
13	[CH2]CCCl mult{2} + [OH3+] + [SHE] --> CCCCl + water	-62.014	-57.808	-58.169	-61.179	-59.159
14	[CH2]CCCl mult{2} + [SHE] --> CC=C + [Cl-]	-60.320	-51.264	-52.068	-56.265	-51.207
15	CC(CCl)Cl + [SHE] --> [CH2]C(C)Cl mult{2} + [Cl-]	-0.143	7.244	7.862	8.299	12.775
16	[CH2]C(C)Cl mult{2} + [OH3+] + [SHE] --> CC(C)Cl + water	-60.211	-56.963	-56.626	-60.412	-58.790

17	[CH2]C(C)Cl mult{2} + [SHE] --> CC=C + [Cl-]	-56.003	-47.821	-47.769	-52.288	-47.594
18	CC(CCl)Cl + 2 [SHE] --> CC=C + 2 [Cl-]	-56.147	-40.577	-39.907	-43.989	-34.819
19	C(CCl)CCl + 2 [SHE] --> CC=C + 2 [Cl-]	-56.980	-41.862	-41.378	-46.121	-36.831
20	CC(CCl)Cl + [SHE] --> C[CH]CCl mult{2} + [Cl-]	-2.495	4.101	4.778	5.831	12.517
21	C[CH]CCl mult{2} + [OH3+] + [SHE] --> CCCCl + water	-55.345	-51.221	-50.786	-54.735	-55.287
22	CC=C + [HH] --> CCC	-18.825	-24.344	-21.476	-20.407	-19.920
23	CCCCl + [SHE] --> [CH2]CC mult{2} + [Cl-]	4.751	10.944	12.477	11.462	15.599
24	[CH2]CC mult{2} + [OH3+] + [SHE] --> CCC + water	-61.390	-57.315	-57.941	-60.670	-58.683
25	CC(C)Cl + [SHE] --> C[CH]C mult{2} + [Cl-]	2.705	9.148	10.282	10.880	15.576
26	C[CH]C mult{2} + [OH3+] + [SHE] --> CCC + water	-56.830	-52.920	-52.991	-56.879	-55.416
27	C(C(CCl)Cl)Cl --> C(=CCl)CCl + HCl	-3.409	2.873	0.119	5.004	2.030
28	C(C(CCl)Cl)Cl --> C(=CCl)(C)Cl + HCl	-3.033	1.971	-0.840	3.841	1.255
29	C(=CCl)CCl + [SHE] --> [H][C]([H])C=CCl mult{2} + [Cl-]	-12.159	-5.910	-4.144	-4.817	-0.011
30	[H][C]([H])C=CCl mult{2} + [OH3+] + [SHE] --> C(=CCl)C + water	-46.803	-43.109	-43.476	-47.018	-45.300
31	C(=CCl)(C)Cl + [SHE] --> CC(Cl)=[CH] mult{2} + [Cl-]	11.438	19.111	20.313	18.384	22.438
32	CC(Cl)=[CH] mult{2} + [OH3+] + [SHE] --> C(=C)(C)Cl + water	-71.995	-68.619	-68.283	-71.028	-69.014
33	C(=CCl)C + [SHE] --> CC=[CH] mult{2} + [Cl-]	14.255	20.778	22.598	20.032	23.970
34	CC=[CH] mult{2} + [OH3+] + [SHE] --> CC=C + water	-71.680	-67.541	-67.762	-70.030	-68.052
35	C(=C)(C)Cl + [SHE] --> C[C]=C mult{2} + [Cl-]	10.855	17.516	18.770	18.059	22.794
36	C[C]=C mult{2} + [OH3+] + [SHE] --> CC=C + water	-67.062	-62.887	-62.624	-66.083	-64.836

[a] Reaction ID No. correspond to those in Figure 2 in the main text. Reaction details are described in Table S1.
[b] Syntax for submission to Arrows. [SHE]: Standard Hydrogen Electrode for electron e^-. mult{}: multiplicity or degeneracy. mult{2}: doublet radical. [OH3+]: hydronium (H_3O^+). [HH]: H_2.

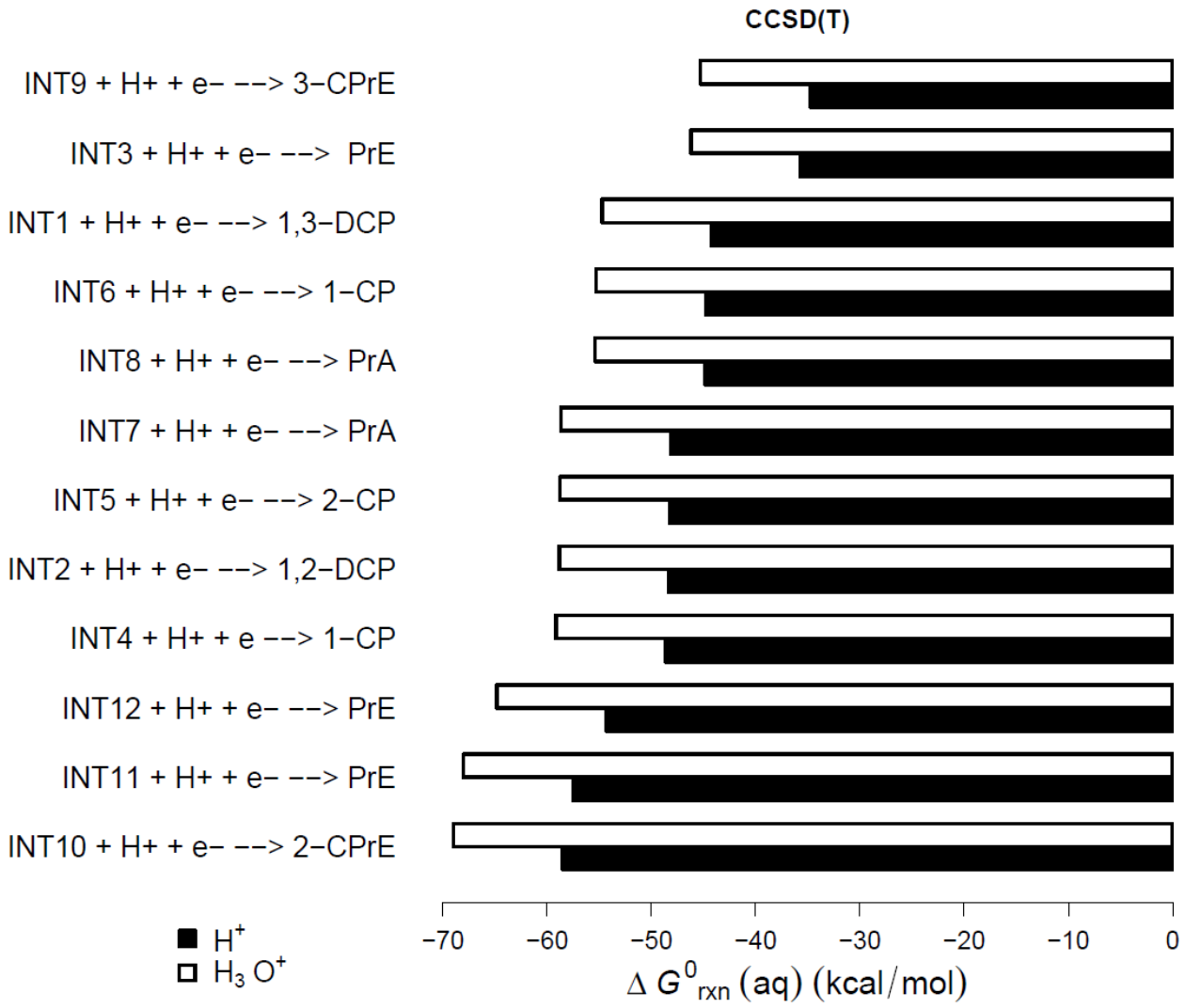

Figure S1 Comparison between hydron (H^+) and hydronium (H_3O^+) models for computationally derived standard state aqueous phase Gibbs free energies (ΔG^0_{rxn} (aq), kcal/mol) of the H-atom attachment (HA) reactions shown in Figure 2 in the main text. Reactions are listed in ascending order of thermodynamic favorability according to the H^+ model starting from the top (i.e., top row for least favorable and bottom row for most favorable).

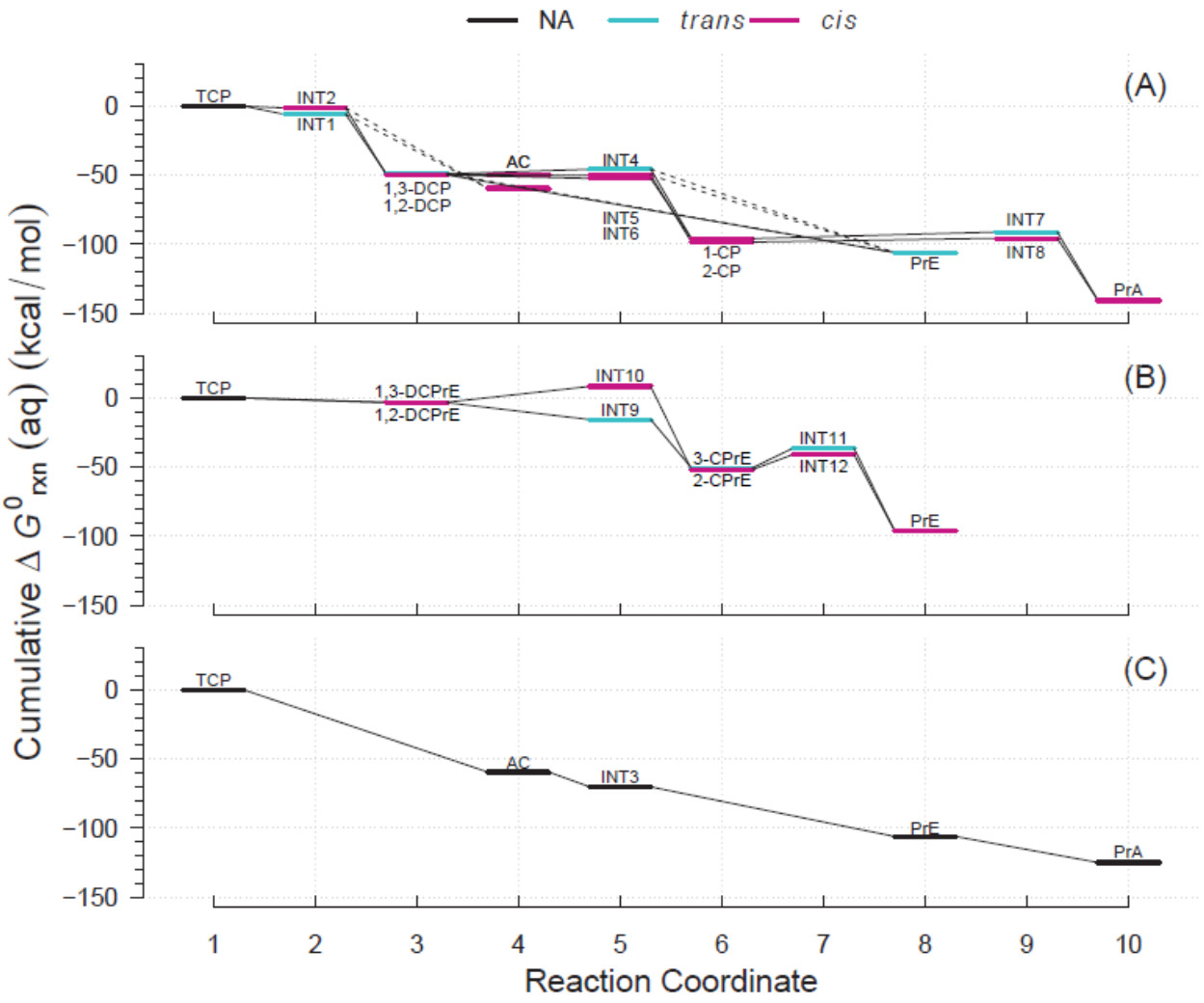

Figure S2 Reaction Coordinate Diagrams (RCDs) with energies computed using DFT with B3LYP for all the reactions shown in Figure 2. (A) Pathway 1: HGL, (B) Pathway 2: DHX, and (C) Pathway 3: BRE + HDG. Reaction coordinate (RC): compound specific, assigned to main reaction products, and incremental with pathway progression (see RCDs sections in main text for details). RCs and abbreviations listed and defined in **Table S1**. Standard state aqueous phase Gibbs free energies (ΔG^0_{rxn} (aq), kcal/mol): cumulative at each RC yielding a pathway energy profile, i.e., a RCD. Colored lines at RC indicate relative molecular structure position of two Cl atoms. Dashed connecting lines indicate reactions of uncertain likelihood. H-atom model used: hydron (H^+) (see Section 3.3 of the main text for details).

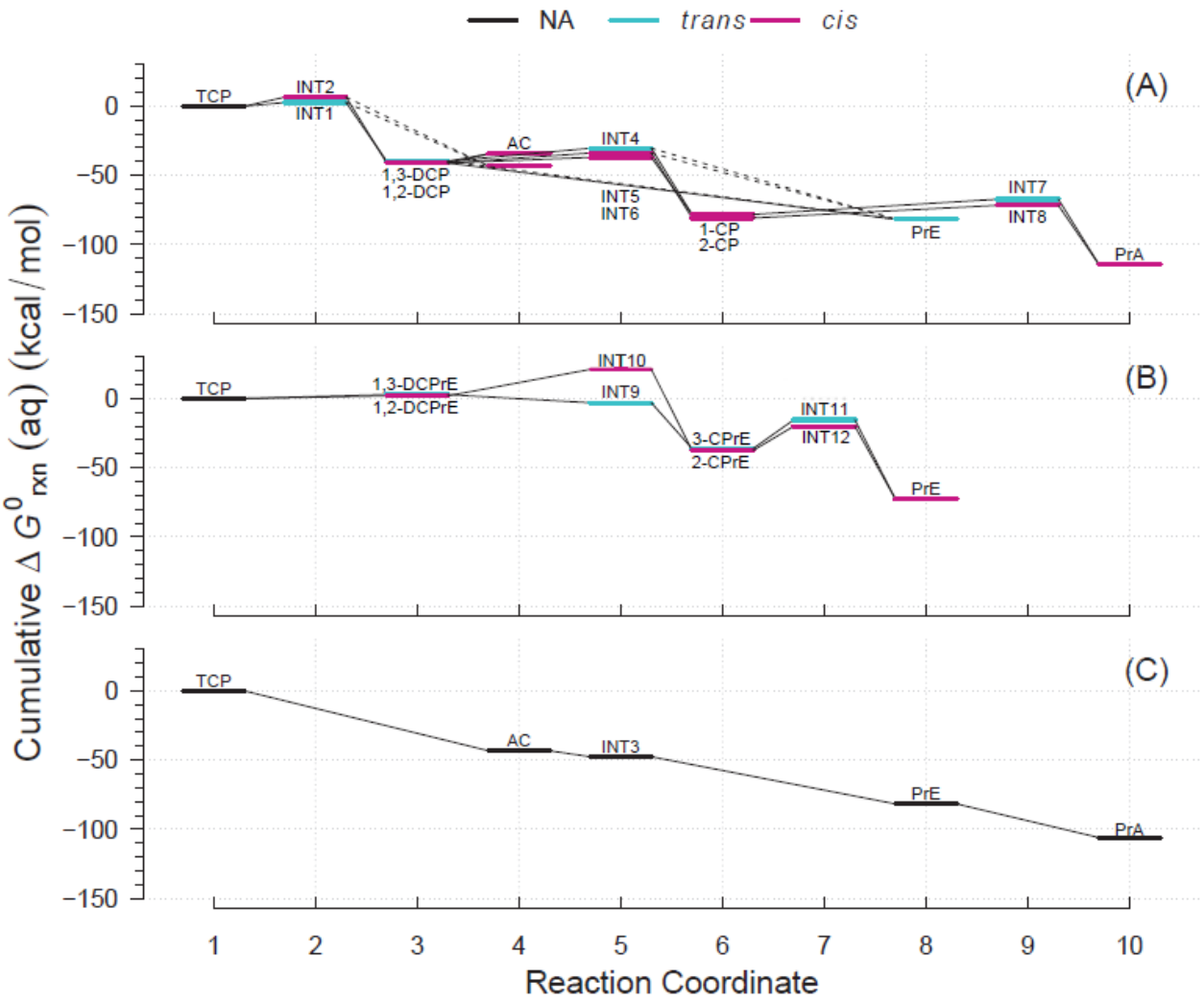

Figure S3 Reaction Coordinate Diagrams (RCDs) with energies computed using DFT with PBE0 for all the reactions shown in Figure 2. (A) Pathway 1: HGL, (B) Pathway 2: DHX, and (C) Pathway 3: BRE + HDG. Reaction coordinate (RC): compound specific, assigned to main reaction products, and incremental with pathway progression (see RCDs sections in main text for details). RCs and abbreviations listed and defined in **Table S1**. Standard state aqueous phase Gibbs free energies (ΔG^0_{rxn} (aq), kcal/mol): cumulative at each RC yielding a pathway energy profile, i.e., a RCD. Colored lines at RC indicate relative molecular structure position of two Cl atoms. Dashed connecting lines indicate reactions of uncertain likelihood. H-atom model used: hydron (H^+) (see Section 3.3 of the main text for details).

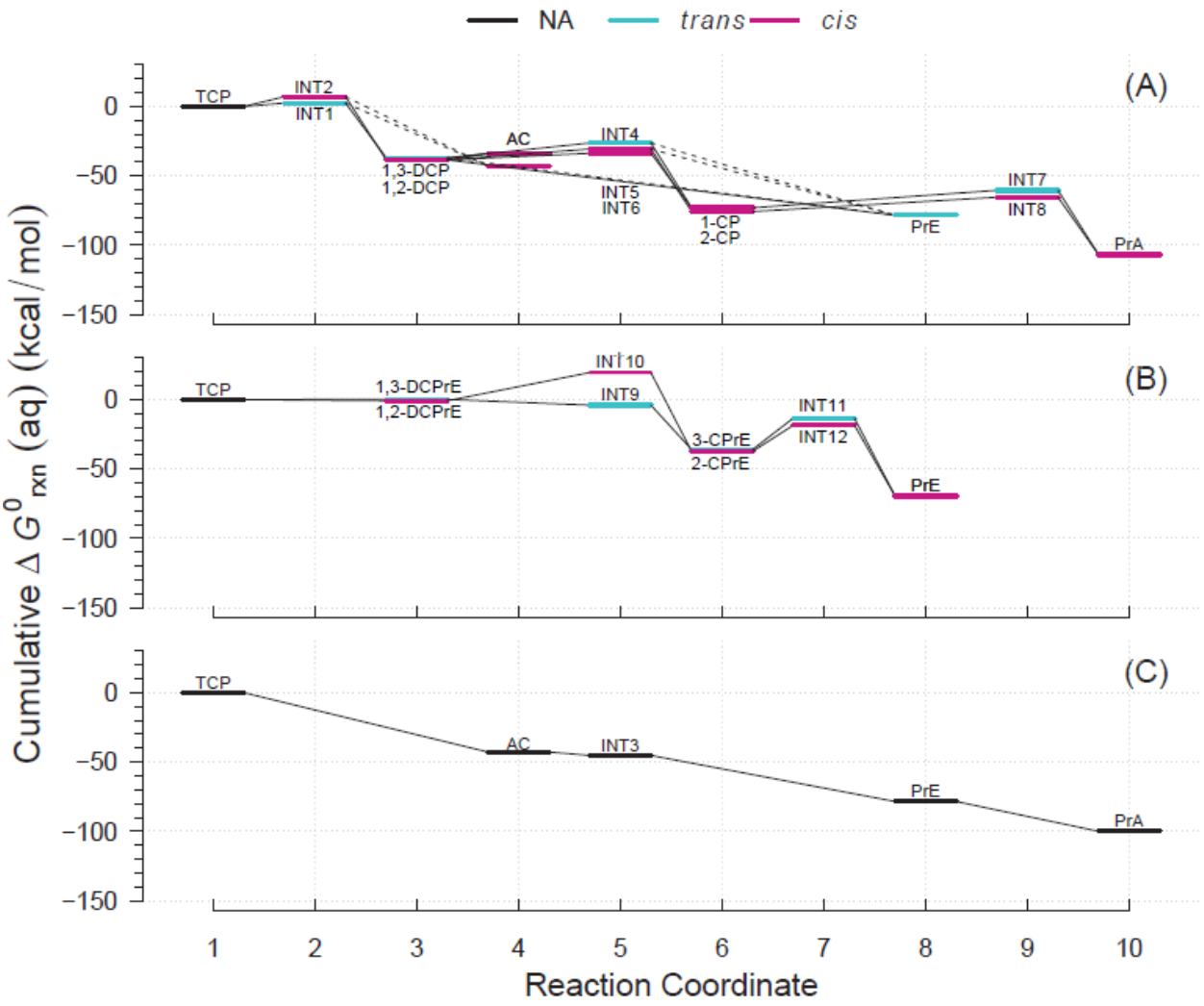

Figure S4 Reaction Coordinate Diagrams (RCDs) with energies computed using DFT with PBE96 for all the reactions shown in Figure 2. (A) Pathway 1: HGL, (B) Pathway 2: DHX, and (C) Pathway 3: BRE + HDG. Reaction coordinate (RC): compound specific, assigned to main reaction products, and incremental with pathway progression (see RCDs sections in main text for details). RCs and abbreviations listed and defined in **Table S1**. Standard state aqueous phase Gibbs free energies (ΔG^0_{rxn} (aq), kcal/mol): cumulative at each RC yielding a pathway energy profile, i.e., a RCD. Colored lines at RC indicate relative molecular structure position of two Cl atoms. Dashed connecting lines indicate reactions of uncertain likelihood. H-atom model used: hydron (H^+) (see Section 3.3 of the main text for details).

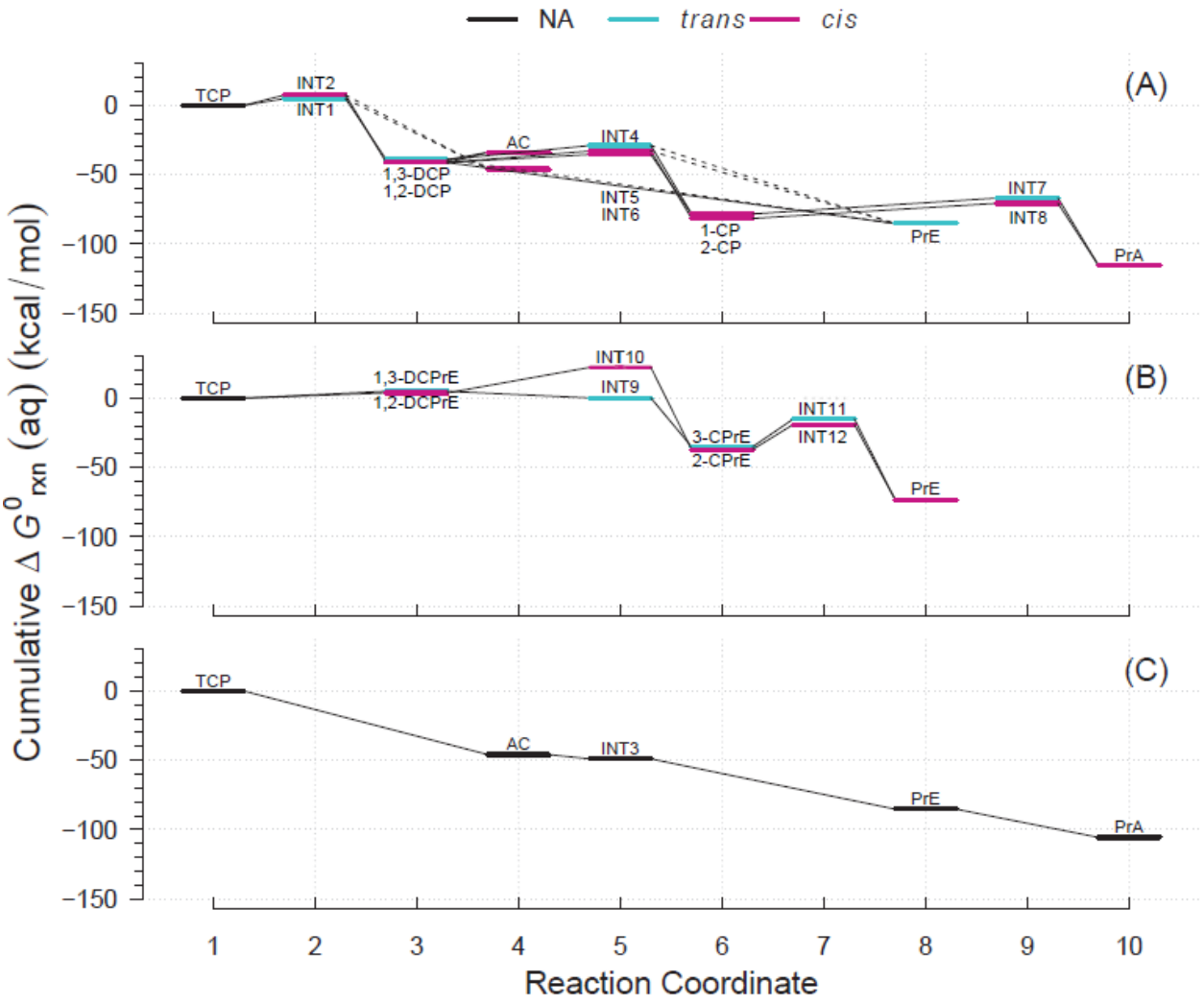

Figure S5 Reaction Coordinate Diagrams (RCDs) with energies computed using DFT with M06-2X for all the reactions shown in Figure 2. (A) Pathway 1: HGL, (B) Pathway 2: DHX, and (C) Pathway 3: BRE + HDG. Reaction coordinate (RC): compound specific, assigned to main reaction products, and incremental with pathway progression (see RCDs sections in main text for details). RCs and abbreviations listed and defined in **Table S1**. Standard state aqueous phase Gibbs free energies (ΔG^0_{rxn} (aq), kcal/mol): cumulative at each RC yielding a pathway energy profile, i.e., a RCD. Colored lines at RC indicate relative molecular structure position of two Cl atoms. Dashed connecting lines indicate reactions of uncertain likelihood. H-atom model used: hydron (H^+) (see Section 3.3 of the main text for details).

Batch Experimental Methods

Reagents. The ZVZ used in this study was an industrial-grade material, Zinc Dust 64 (Horsehead Corporation, Monaca, PA). ZVZ was used as received. Saturated stock solutions of 1,2,3-trichloropropane (>98%, Fluka) , 1,2-dichloropropane (99+%, Aldrich), 1,3-dichloropropane (98+%, TCI), and allyl chloride (99+%, TCI) were prepared in deionized (MilliQ) water. Deioinized (DI) water was used without further treatment.

Batch Experiments. Batch reactor experiments were performed in 160-mL or 120-mL serum vials sealed with Hycar® septa (Thermo Scientific) and aluminum crimp caps. Reactors were filled with the appropriate amount of ZVZ and DI water to achieve ZVZ load of 250 g/L. All batch reactors (including those used in calibration) contained a 1:1 ratio of liquid to headspace (necessitated by the high rate of hydrogen production due to ZVZ reduction of water). Before addition of chlorinated solvent, reactors were "pre-exposed" at room temperature for 20-28 hours (to allow equilibration of the oxide layer on ZVZ with the solution conditions) while rotating end-over-end at ~9 rpm. Following pre-exposure, experiments were initiated by injection of a saturated aqueous stock solution. Batch reactors were then rotated end-over-end at ~32 rpm for the duration of experiment.

Analysis. Aqueous aliquots and headspace samples from batch reactors were analyzed by gas chromatography (GC). Aqueous aliquots (1 mL) were removed from the batch reactor and extracted with an equal volume of hexane, which was directly injected on an Agilent 5890 Series II GC equipped with a DB-624 column (J&W/Agilent) and electron capture detector (for analysis of chlorinated species). Concentrations were determined through comparison to calibration curves prepared by analyzing batch reactors containing various concentrations of chlorinated solvent in DI water. Headspace samples (500 μL) were removed from batch reactors with a gas tight syringe and directly injected on an Agilent 5890 GC equipped with a flame ionization detector (for analysis of propene). Concentration were determined though comparison to known concentrations prepared in Tedlar bags.

Batch Experimental Results

Data Fit and Normalization. Concentration versus time data were fit to a pseudo-first-order model to obtain an observed rate constant (k_{obs}). These data were normalized to the surface area concentration of ZVZ (using specific surface areas obtained by BET N_2-gas adsorption) to obtain a surface-area-normalized rate constant (k_{SA}). The surface area of Zinc Dust 64 was assumed to be 0.620 m^2/g.[25] Concentration versus time plots for the disappearance of TCP, 1,2-DCP, 1,3-DCP, and allyl chloride and appearance of propene are shown in **Figure S6**. No other products or intermediates were detected. Corresponding k_{obs} and k_{SA} values are given in **Table 1**.

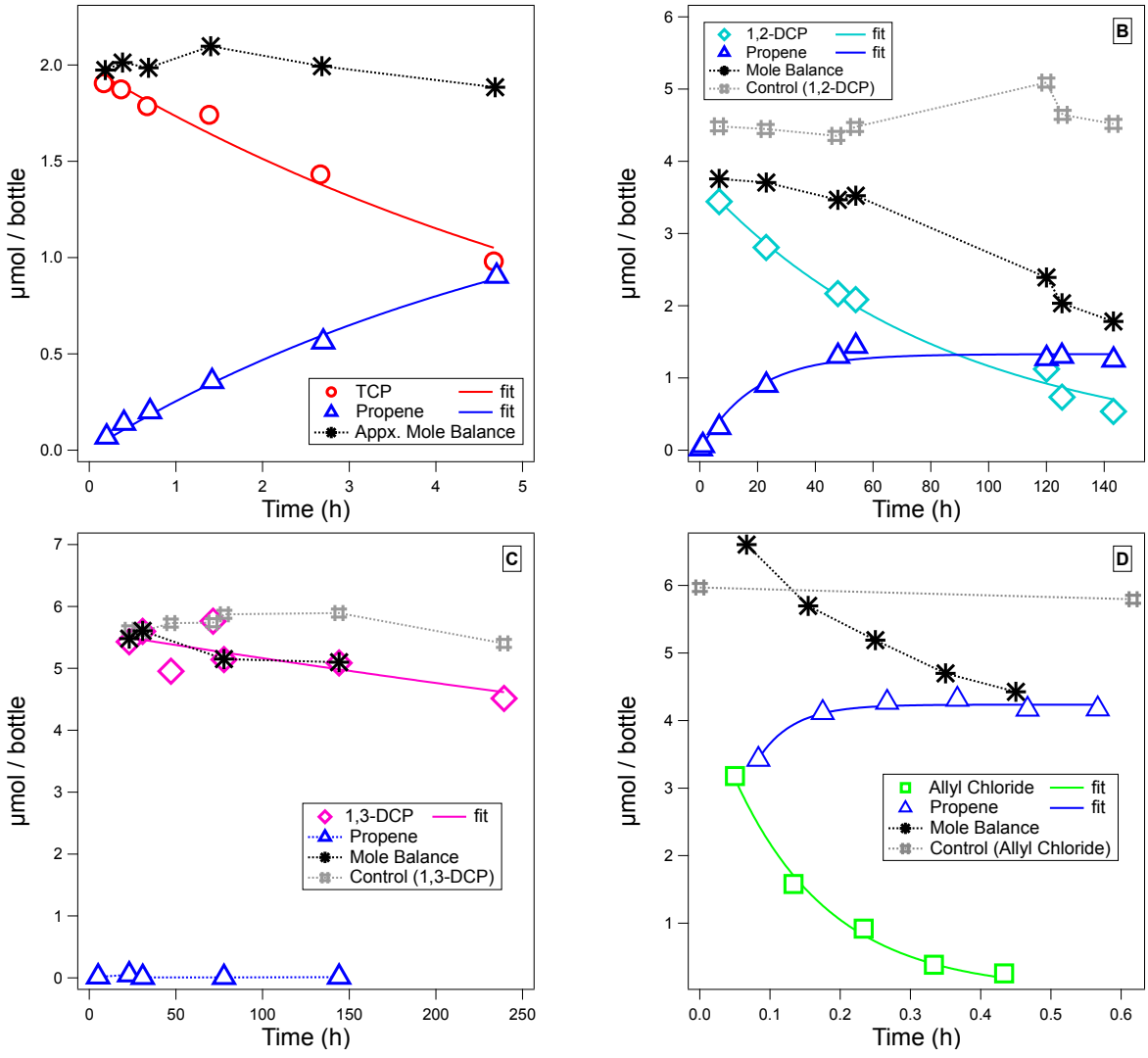

Figure S6. Disappearance of (a) TCP, (b) 1,2-DCP, (c) 1,3-DCP, and (d) allyl chloride and appearance of propene over time in the presence of ZVZ. Where possible, data for the disappearance of parent compounds and appearance of propene were fit independently to a first order model.

Because no measureable quanitites of intermediates were detected during TCP batch experiments, a separate batch experiment was performed with a high initial concentration of TCP. Aqueous alliqots were anlayzed as described above using GC with electon capture detection to detect potential chlorinated products. Results are presented in **Figure S7**. Allyl chloride was the only detected intermediate. Concentrations of allyl chloride were too low to be accurately fit; however, they were used to validate subsequent modeling.

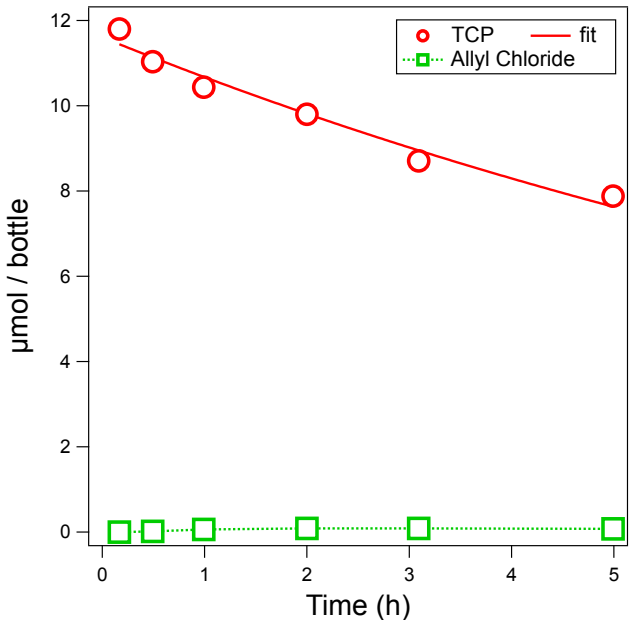

Figure S7. Disappearance of TCP and appearance of allyl chloride in the presence of ZVZ.

Kinetic modeling. In order to better understand the kinetics of allyl chloride generation and degradation, the kinetics of TCP reduction to allyl chloride and subsequent reduction of allyl chloride to propene were modeled assuming consecutive first-order behavior. The closed form solution to the rate laws for this system[26] is given by equations S2-S4,

$$[TCP] = [TCP]_0 e^{-k_1 t} \tag{S2}$$

$$[AC] = \frac{k_1[TCP]_0}{k_2 - k_1}\left[e^{-k_1 t} - e^{-k_2 t}\right] \tag{S3}$$

$$[P] = [TCP]_0\left[1 - \left(\frac{k_2}{k_2 - k_1}\right)e^{-k_1 t} + \left(\frac{k_1}{k_2 - k_1}\right)e^{-k_2 t}\right] \tag{S4}$$

where [TCP], [AC], and [P] are the concentrations of TCP, allyl chloride, and propene at time t, $[TCP]_0$ is the initial concentration of TCP in the reactor, and k_1 and k_2 are the rate constant for the first and second reaction steps. The model was parameterized with the TCP and allyl chloride rate constants obtained in this study (tabulated in **Table 1**) and an assumed initial TCP concentration of 1 µmol/bottle (the µmol/bottle concentration convention was used to account for mass in both the aqueous phase and headspace).

The results of this model are shown in **Figure S8** along with experimental data normalized to the initial concentration of TCP (as shown in **Figures S6a** and **S7**). The model and experimental data for appearance/dissappearance of allyl chloride and appearance of propene show excellent agreement, supporting the assumed kinetic model: consecutive first-order reduction of TCP to allyl chloride to propene.

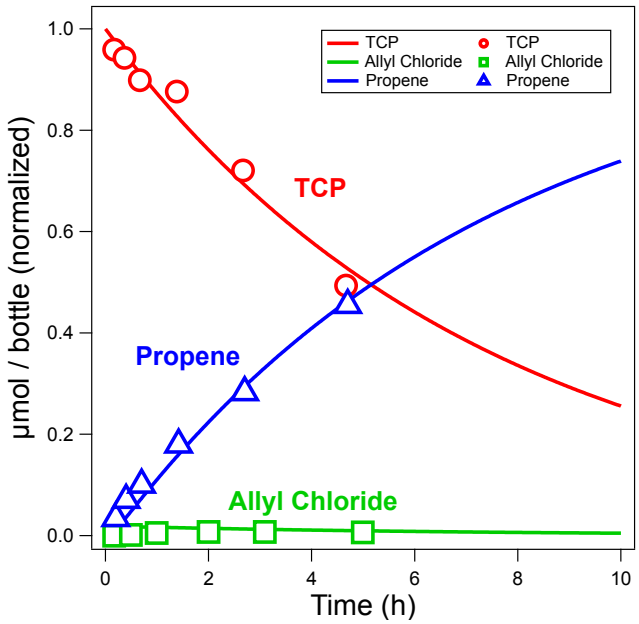

Figure S8. Consecutive first-order reaction model for TCP → allyl chloride → propene. The model assumes TCP and allyl chloride disappearance rates as reported in Table 1. Also shown are empirical data for TCP disappearance and propene appearance (as shown **Figures S6a**) and empirical data for the appearance and disappearance of allyl chloride (as shown in **Figure S6d**). All data have been normalized to the fitted initial concentration of TCP in the respective experiment.

References in Supporting Information

1. A. D. Becke. Density-functional thermochemistry. III. The role of exact exchange. *J. Chem. Phys.*, 1993, **98**, 5648-5652 [DOI 10.1063/1.464913].

2. C. Lee, W. Yang and R. G. Parr. Development of the Colle-Salvetti correlation-energy formula into a functional of electron density. *Phys. Rev. B*, 1988, **37**, 785-789.

3. C. Adamo and V. Barone. Toward reliable density functional methods without adjustable parameters: The PBE0 model. *J. Chem. Phys.*, 1999, **110**, 6158.

4. J. P. Perdew, K. Burke and M. Ernzerhof. Generalized gradient approximation made simple. *Phys. Rev. Lett.*, 1996, **77**, 3865.

5. Y. Zhao and D. G. Truhlar. The M06 suite of density functionals for main group thermochemistry, thermochemical kinetics, noncovalent interactions, excited states, and transition elements: two new functionals and systematic testing of four M06-class functionals and 12 other functionals. *Theor. Chem. Acc.*, 2008, **120**, 215-241.

6. R. J. Bartlett and J. F. Stanton. Applications of Post-Hartree—Fock Methods: A Tutorial. In *Reviews in Computational Chemistry*, eds. K. B. Lipkowitz and D. B. Boyd, Wiley, 1994, vol. 5, pp. 65-169 [DOI 10.1002/9780470125823.ch2].

7. R. J. Bartlett and M. Musiał. Coupled-cluster theory in quantum chemistry. *Rev. Mod. Phys.*, 2007, **79**, 291.

8. T. Clark, J. Chandrasekhar, G. W. Spitznagel and P. v. R. Schleyer. Efficient diffuse function-augmented basis sets for anion calculations. III. The 3-21+G basis set for first-row elements, Li to F. *J. Comput. Chem.*, 1983, **4**, 294-301 [DOI 10.1002/jcc.540040303].

9. R. Krishnan, J. S. Binkley, R. Seeger and J. A. Pople. Self-consistent molecular orbital methods. XX. A basis set for correlated wave functions. *J. Chem. Phys.*, 1980, **72**, 650-654 [DOI 10.1063/1.438955].

10. G. Herzberg, *Molecular Spectra and Molecular Structure III. Electronic Spectra and Electronic Structure of Polyatomic Molecules*, Van Nostrand, Princeton, NJ, 1966.

11. D. A. McQuarrie. Statistical Mechanics. 1973.

12. A. J. Salter-Blanc, E. J. Bylaska, H. Johnston and P. G. Tratnyek. Predicting reduction rates of energetic nitroaromatic compounds using calculated one-electron reduction potentials. *Environ. Sci. Technol.*, 2015, **49**, 3778–3786 [DOI 10.1021/es505092s].

13. A. Klamt and G. Schüürmann. COSMO: A new approach to dielectric screening in solvents with explicit expressions for the screening energy and its gradient. *J. Chem. Soc., Perkin Trans. 2*, 1993, 799-803.

14. E. V. Stefanovich and T. N. Truong. Optimized atomic radii for quantum dielectric continuum solvation models. *Chem. Phys. Lett.*, 1995, **244**, 65-74.

15. R. A. Pierotti. Aqueous solutions of nonpolar gases. *J. Phys. Chem.*, 1965, **69**, 281-288.

16. F. M. Floris, J. Tomasi and J. L. Pascual Ahuir. Dispersion and repulsion contributions to the solvation energy: Refinements to a simple computational model in the continuum approximation. *J. Comput. Chem.*, 1991, **12**, 784-791.

17. B. Honig, K. A. Sharp and A. Yang. Macroscopic models of aqueous solutions: Biological and chemical applications. *J. Phys. Chem.*, 1993, **97**, 1101-1109.

18. J. Tomasi and M. Persico. Molecular interactions in solution: An overview of methods based on continuous distributions of the solvent. *Chem. Rev.*, 1994, **94**, 2027-2094.

19. D. Sitkoff, K. A. Sharp and B. Honig. Accurate calculation of hydration free energies using macroscopic solvent models. *J. Phys. Chem.*, 1994, **98**, 1978-1988.

20. C. J. Cramer and D. G. Truhlar. Implicit solvation models: Equilibrium, structure, spectra, and dynamics. *Chem. Rev.*, 1999, **99**, 2161-2200.

21. F. Eckert and A. Klamt. Fast solvent screening via quantum chemistry: COSMO-RS approach. *AIChE J.*, 2002, **48**, 369-385.

22. M. J. Huron and P. Claverie. Calculation of the interaction energy of one molecule with its whole surrounding. II. Method of calculating electrostatic energy. *J. Phys. Chem.*, 1974, **78**, 1853-1861.

23. A. Ben-Naim and Y. Marcus. Solvation thermodynamics of nonionic solutes. *J. Chem. Phys.*, 1984, **81**, 2016-2027 [DOI 10.1063/1.447824].

24. A. Shrake and J. A. Rupley. Environment and exposure to solvent of protein atoms. Lysozyme and insulin. *J. Mol. Biol.*, 1973, **79**, 351-364.

25. A. J. Salter-Blanc and P. G. Tratnyek. Effects of solution chemistry on the dechlorination of 1,2,3-trichloropropane by zero-valent zinc. *Environ. Sci. Technol.*, 2011, **45**, 4073-4079 [DOI 10.1021/es104081p].

26. C. Capellos and B. H. J. Bielski, *Kinetic Systems: Mathematical Descriptions of Chemical Kinetics in Solution*, Wiley, New York, 1972.